

Detection of Brain Tumor using Transfer Learning using Conventional Autoencoder with Long Short Term Memory method

D Agalya, Research Scholar
Department of Computer Science
School of Computing Sciences
Vels Institute of Science, Technology & Advanced Studies
Pallavaram, Chennai, India
agalya888@gmail.com

Dr.S. Kamalakkannan, Professor
Department of Information Technology
School of Computing Sciences
Vels Institute of Science, Technology & Advanced Studies
Pallavaram, Chennai, India
kannan.scs@vistas.ac.in

Abstract— Brain tumor (BT) has generate a significant health challenge by putting pressure on healthy brain parts or spreading into other areas as well as blocking the flow of fluid around the brain. BT diagnosis is an extensive and time consumption process that depends primarily on radiologists experience and interpretive capabilities. For the area of medical imaging, automatic segmentation of images by means of Deep Learning (DL) approaches. The DL approaches assist in transforming the sector, resulted in improving precision and effectiveness of investigations. However, there are various feature extraction mechanisms available. Therefore, the Recurrent Neural Network (RNN) is utilized for feature extraction and image classification. In model execution, the data have trained in transforming the test image as well as data features for minimizing the domain shift is calculated through the Convolutional Autoencoder (CAE) for reconstruction loss. This research has concentrated in building a model with VGG16 as a single test that subjected at inference and existing method is adopted as neural networks for AE as Transfer Learning (TL) that performs an image analysis task such as segmentation and even set as an adopter for pre training the model. The AE used to train from the source dataset and perform as the adaptors in optimizing during testing using a test subject for effective computation. Moreover, the Long Short Term Memory (LSTM) is utilized as RNN model with CAE for providing improved detection of BT in healthcare industries. Hence, the proposed CAE with LSTM is compared with AE with Convolutional Neural Network (CNN) for evaluating BT detection using MRI dataset with various BT type classifications.

Keywords: *Transfer Learning, Convolutional Autoencoder, Brain tumor, Long Short Term Memory, Deep Learning.*

I. INTRODUCTION

Brain and spinal cord is utilized for composing human central nervous system in the human body [1]. Analysis, integration, organisation, decision-making, and sending commands to the body are among the biological functions that are primarily controlled

through brain whereas human brain's anatomical complexity is incredible [2]. It can be challenging to identify, evaluate, and treat some CNC issues, such as infection, BT, headaches and stroke [3]. The brain is surrounded by hard skull contains aberrant cell growths called BTs [4]. Complications may arise from growth in even small space of the brain. Any tumour in the skull has the potential to harm the brain, which makes it extremely dangerous. In general, mortality rate is ranked as tenth for BT and abnormal growth of nerve cells has resulted in an accumulation is the BT characteristic [5]. The brain and central nervous system can produce over 130 distinct types of tumours, from benign to malignant as well as from exceedingly complexity to prevalent [6]. These cancers can develop in the brain as primary BT or spread to other parts of the body is said to be metastatic BT. The term primary BT describes tumours that start inside the brain. These tumours might be enclosed in the nerve cells which surround the brain or they can be produced from brain cells. There are several types of primary BT, including benign and malignant ones. The most prevalent kind of malignant BT are secondary BT, sometimes referred to as metastatic BT. Notably, secondary BT are always malignant and represents a major risk to health, whereas benign tumours usually do not move from one part of the body to another [7]. Nearly, 700,000 of individual with primary BT in United States and almost 85,000 new instances of BT were identified in the US alone during 2021. When a BT is present, a number of factors influence the prognosis and survival rates, including the patient's age. According to the study, one year survival rate for patients between the ages of 55 and 64 is 46.1% and in the case of patients between the ages of 65 and 74 is 28.3% [8]. Early tumour diagnosis is crucial for improving the chance of survival [9].

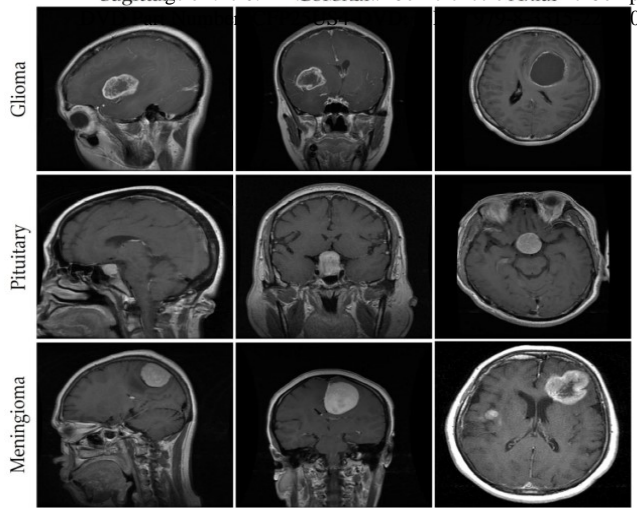


FIGURE 1 TYPES OF TUMOR WITH MRI IMAGES FROM THE BT DATASET

Gliomas, pituitary tumours, and meningiomas are the most common primary BT observed in clinical practice, as illustrated in Figure 1 [10]. Nearby meningeal tissues on the spinal cords periphery or brain, meningiomas often develop. The membranes assist in protecting the spinal cord and brain are where this benign tumour develops. However, the glial cells that support and envelop the neurones give rise to gliomas, the BT with the greatest mortality rate. Gliomas make up for one-third of all BT cases. The pituitary gland is the site of benign pituitary tumour development [11]. A proper diagnosis determines the lifespan and available treatments for BT.

Researcher majorly focuses on three different tumours namely pituitary, meningioma, and gliomas [12] [13]. A promising and quickly expanding area is Artificial Intelligence (AI). Giving the machine the capacity to think like a human is the goal. In the data-driven discipline of Machine Learning (ML), machines are given the capacity to learn without explicit programming. This field is being widely applied in medicine, particularly in medical imaging [14]. DL is the area of ML that performs the best when compared to supervised learning. The usage of Artificial Neural Networks (ANN) as an algorithm, which simulates the functioning of the human brain, is the domain's advantage. The majority of this work involve image processing using computer vision field, where images are the ML foundation. Breast cancer is classified as either benign or malignant with respect to characteristics of a Modified Recurrent Neural Network (MRNN). The outcome of proposed model determines that existing models already in use have yield with 86% accuracy in detection of breast cancer. Thus, the proposed DL method involves a huge number of parameters, which complicates computation [15]. The BT detection and classification of BT types are potentially be aided by a method developed from the performances of DL. Creating the sequential method canable to identify discriminate among brains with and without tumours but the different among types of tumours will be a challenge. Hence, the proposed DL model with TL is used to identify the BT detection precise than existing methods.

II. LITERATURE REVIEW

Nazir et al., have provided a thorough analysis of the current research and findings, in order to more accurately identify and classify brain cancers using MRI images. This study will be particularly helpful for DL experts who wish to utilise their knowledge to classify and identify BT [16]. Satpute et al., have executed an analysis with CNN-based technique for BT using MRI data segmentation. There are currently several categorisation and prediction techniques for diagnosing BT. An in-depth analysis is provided on the advantages and disadvantages of current brain tumor diagnostic methods. To overcome these limitations, a classifier based on Convolutional Neural Networks (CNNs) is suggested. When a CNN-based classifier is used to compare the training and testing data, the best outcome is achieved [17]. Using a dataset created from 3D BRATS pictures, Kabir et al., have presented a technique for brain cancer detection and classification that can reliably identify if a tumour is present or not in the MRI image using 217 BRATS dataset and justify the BT whether it is benign or malignant. The recommended method includes image pre-processing and segmentation with enhancement of multi-valued threshold as well as feature extraction and selection for generating classification process using various models. The proposed method has been tested for both the original BRATS dataset as well as improved edition of the same dataset [18].

Hameed et al., have used a lot of data to train DL models in order to automatically classify complicated photos of cancer cells. The CNN and RNN merits are combined [19]. Yan et al., have employed a neural network to analyse photos of breast cancer histology. A CNN was used to obtain higher hierarchical information from case images, and an RNN was used to fuse plaque characteristics to determine the final image classification. However, a lot of redundant features must be processed by the majority of feature extraction methods [20]. Feng et al., have introduced an autoencoder designed to preserve the manifold structure. This method first extracts discriminate features from unlabeled data. It then refines the NN by using labelled data, ensuring the input dataset's structure remains intact from a classical learning standpoint. Additionally, it focuses on minimizing reconstruction errors across extensive unlabelled data, which facilitates the extraction of discriminative features within the DL framework. Graph representations may be challenging to discern due to the intricacy of label connections in pictures [21]. Nguyen et al., have introduced the Modular Graph Transformer Network (MGTN) has separates a computation graph into various subgraphs with modular-based through preprocessing approach, allowing distinct subgraphs to transmit information more effectively [22]. Wang et al., have developed a method for BC classification using histopathological images by integrating a transformer model with contrastive learning. This approach employs a novel two-channel structure to extract both convolutional and capsule features simultaneously. By merging the advantages of CNN and capsule networks, it enhances feature fusion and augmented routing [23]. Tilagaraj et al., have a Deep CNN and an artificial fish swarm algorithm were combined, and an enhanced DCNN for categorisation of BC images by an

artificial fish schooling model was proposed. The Artificial fish and swarm algorithm directly provides the train data for the DCNN [24]. Hong et al., have proposed the spectral former, which overcomes the limitations of traditional CNN by utilizing the inherent network backbone of transformers. This approach addresses the challenges typically associated with the order of transformers [25]. Liu et al., have introduced a Bayesian neural network-based hierarchical learning approach. It constructs a label tree representing visual confusion from the convolutional neural network's results, and then organizes the categories of an image dataset into a hierarchical framework. This method also automatically determines the appropriate tasks for hierarchical learning [26].

This session illustrates and summarise the CNN based techniques for BC and BT detection as well as find out the less precision in BT detection is identified as the limitation for diagnosing diseases from medical imaging. Moreover, the benefits of RNN and AE are discussed for better detection of medical imaging with better diagnosis of diseases. Thus, the RNN with AE is considered as proposed model in this research.

III. RESEARCH METHODOLOGY

This research focus on improving the classification accuracy for better detection of BT that can be done through the feature extraction method named CAE which is implemented with RNN model as LSTM. The image dataset is fed into the CAE and the pretrained CAE output has been utilized as the input to LSTM for fine-tuning the model. Moreover, CAE assist in considering the significant features from the available images as an input and the classification accuracy get accomplished. Figure 2 illustrate the overall architecture of predicting BT using CAE with LSTM model.

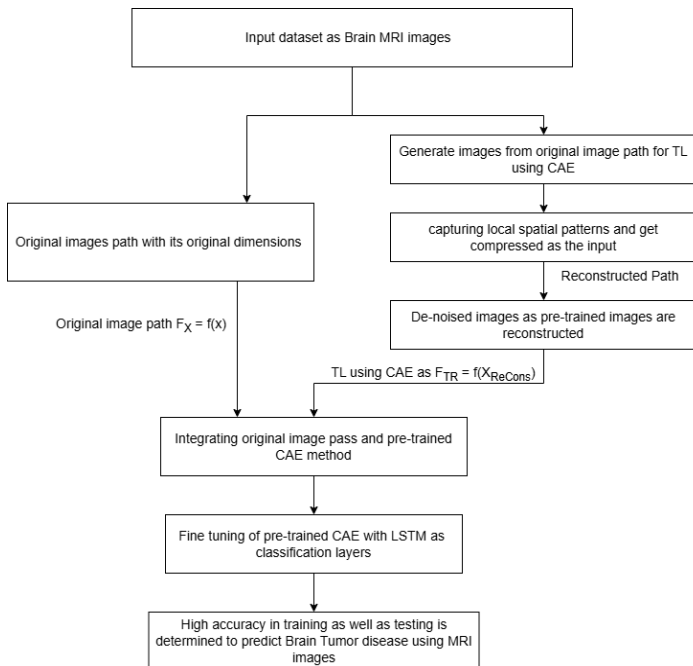


FIGURE 2 ARCHITECTURE OF PREDICTING BT USING CAE WITH LSTM

This architecture is implemented with generating clone image as auxiliary image from the original image to implement with TL using CAE technique. There are two different path as original image path and image path whereas the auxiliary image is extracted with VGG16 layer as Relu layer and 2D conv layer for capturing the local spatial pattern and compressed as an input as reconstructed path. Moreover, the de-noised images are pre-trained images that get reconstructed using CAE concept and made integrated as mapping with original images. Finally, the pre-trained CAE method images are fine tuned with LSTM classification layers for better feature extraction for generating high accuracy in predicting BT class classification in diagnosis.

IV. DATA COLLECTION AND DATA PREPROCESSING

Most of the primary CNS tumor is considered to be BT and it is diagnosed from 11,700 individuals from every year. The survival rate of 5-years with CNS tumors or cancerous brain for men and women are 34% and 36% respectively. According to the dataset collected for types of BT with Magnetic Resonance Imaging (MRI) images have classified as Benign, Malignant and pituitary. The total image files collected from four categories namely no_tumor, glioma_tumor, pituitary_tumor and meningioma_tumor consists of 3264 files. The image size is 495x619 and data with huge amount have been generated via scanned data and radiologist have assisted to examine the generated images. Error prone may occur in manual examination because of level complexities in identifying the BT and its properties. In this research, the MRI image files for four different categories of tumor is segregated with training and testing as 88% and 12% of image files. The improved accuracy of diagnosing the BT type can be done through by understanding the MRI images clearly. The best techniques for detecting BT using automate classification technique using Deep Learning (DL) for proper treatment for enhancing the patient's life expectancy.

Working of CAE

The suggested CAE structure of architecture is shown in Figure 3, which represents the output image as compressed as CAE image datasets as reconstructed images. Moreover, the proposed CAE have utilized Rectified Linear Unit (ReLU) function as an activation function is done once four batches of both 2D convolutional as well as deconvolutional layers at the symmetric architecture. The process that reverses the convolutional layer's function is called deconvolution, or transposed convolution. The input is specifically mapped from the space of low-dimensional to high-dimensional images.

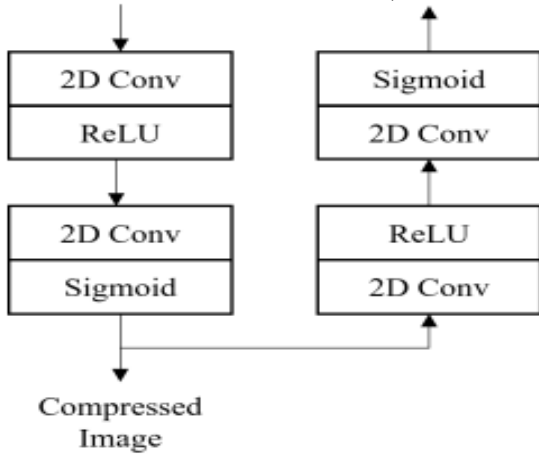


FIGURE 3 TOPOLOGY OF CAE

To be more precise, the first layer (2D Conv1-ReLU1) receives the original input images as dimensions $(H \times W \times 3)$. The process generates 32 down sampling by spatial feature map's using 32 filters as well as dimensions with $H/2 \times W/2$ and this process is said to be CAE Encoder's. Subsequently, the next layer is 2D Conv2-ReLU2 that assists in receiving this output from the encoder and utilizes 2×2 kernel size along with 3 different filters to produce a compressed picture representation with dimensions of $H/4 \times W/4 \times 3$. It makes sense to use a kernel with a lesser size in the second layer as the output feature maps of the first layer have smaller dimensional sizes than the input image. Likewise, the opposite operation of the encoder is carried out symmetrically by the third as well as fourth layers is 2D Deconv3-ReLU3 and 2D Deconv4-ReLU4 corresponding for the components of CAE's decoder.

Algorithm for CAE

Input: Generation amount (Gn), Mutation probability (m), Children size (μ), Training set (T_i), Validation set (V_i)

Output: CAE architecture to find best parent

Step 1- Initialize the parent with number of generation as Gn.

Step 2- Training the model with T_i and assigning the model fitness as F_p using the set V_i .

Step 3- When generation $<$ Gn then do

Step 4- for $i = 1$ to λ do $children_i \leftarrow$ Mutation(parent, m)

$model_i \leftarrow$ Train(children_i, T_i)

$fitness_i \leftarrow$ Evaluate(model_i, V_i)

end for

Step 5- Calculating the fitness of μ to find the best parents with generation Gn

$best \leftarrow \text{argmax}_{i=1,2,\dots,\mu} \{fitness_i\}$

$parent \leftarrow children_{best}$ $F_p \leftarrow fitness_{best}$

else

$parent \leftarrow$ Modify(parent, m)

end if

$G_n = G_n + 1$

Step 6- Repeat step 4 and step 5 until the step 3 meets

Step 7- Return

LSTM working principle

LSTMs are members of the RNN family, which are NNs designed to handle sequential data by sharing internal weights throughout the sequence. LSTM overcomes the decreasing error gradient challenge and preserves long-term dependencies by maintaining the error gradient through its gates.

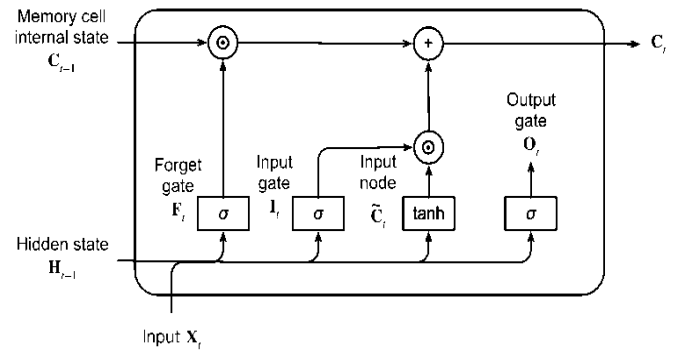


FIGURE 4 ARCHITECTURE OF LSTM MODEL COMPUTATIONS

Where,



- Activation function with FC layers



- Element-wise operators

LSTM method calculation is expressed mathematically has shown in equation 1.

$$h_t = f(W_h * x_t + U_h * h_{t-1} + b_h) \quad (1)$$

Where,

x_t = Current feature embedding

V_h and U_h = feature weight matrix

that imported from the keras application module. The constructor of the neural network with conventional VGG16 layer involves three major arguments namely include_top, input_shape and weight. This network can generate input sizes with weight constructor that mentioned the threshold weight obtain from proposed model such as include_top is involved a classifier with dense connections at the network top as well as input_shape perform an image tensor shape. The image is further fine tuned with LSTM after the CAE is involved. The total image files collected from four categories namely no_tumor, meningioma_tumor, pituitary_tumor and glioma_tumor consist of 3264 files. The image size is 495x619 and data with huge amount is generated through the scans.

TABLE I TRAINING AND TESTING IMAGES OF BT DATASET

BT dataset	BT status	Image Count	Training Images	
			Training	Validating
	No tumor	500	395	105
	Meningioma tumor	937	822	115
	Pituitary tumor	901	827	74
	Glioma tumor	926	826	100

This research majorly focuses for involving CAE instead of involving hyperparameter with huge amount of images and the CAE focuses on providing convolution layers with 3 x 3 filter using a three stalk with maxpooling each as well as frequent utilization of the similar padding to 2 x 2 convolution layer filter with maxpool every to two stalks. The arrangement has done sequence with convolution layer monitored through one layer of max pool for every stalk frequently done by the whole architecture. Finally, it consists of 3 FC layers as dense layer subsequently a softmax for output. The CAE involves conventional layers through weights. The classification of BT tumor with glioma tumor, meningioma tumor and pituitary tumor is clearly defined through CAE with LSTM model for fine tuning the model with best performance in identifying the BT precisely.

The suggested CAE with LSTM model defines the classification of no_tumor, meningioma_tumor, pituitary_tumor and glioma_tumor whereas figures 5 and 6 show the associated model loss as well as training and validation accuracy.

$$b_h = \text{Bias of the feature}$$

Generally, the model consider tanh and ht as the basic hidden state whereas the input gate, forgot gate and output gate is shown in equation 2 to equation 6.

$$f_t = \sigma(V_f * x_t + U_f * h_{t-1} + b_f) \quad (2)$$

$$i_t = \sigma(V_i * x_t + U_i * h_{t-1} + b_i) \quad (3)$$

$$o_t = \sigma(V_o * x_t + U_o * h_{t-1} + b_o) \quad (4)$$

$$c_t = f_t * c_{t-1} + i_t * \tanh(V_c * x_t + U_c * h_{t-1} + b_c) \quad (5)$$

$$h_t = o_t * \tanh(c_t) \quad (6)$$

Where,

h_t = Input gate

f_t = Forget gate

c_t = Memory cell

σ = sigmoid function

O_t = Hadamard product

The forget gate randomly chooses which past information ought to be forgotten, whereas the input gate regulates what newly acquired data is required to remain in the memory cell. Finally, the output gate determines how much data from an internal memory cell will be exposed. These gate units aid an LSTM model in remembering essential data across numerous time steps as automatic segmentations.

The pattern of mutated generation is considered to be the childbest as fitnessbest with reconstruction path of CAE output as TL for the BC class detection dataset. The obtained CAE output is considered to be input for RNN based LSTM method to fine tune the dataset with better feature extraction of Relu as activation function. The sigmoid functions with FC layers are assisting in identifying the precise feature to identify the class precisely.

V. RESULT AND DISCUSSION

In this research, the experiment with high performance server have considered due to image processing whereas 16GB RAM is used with CPU as Core i7 DMI2, storage with 256 GB ROM. The operating system utilized in this experimental research is Ubuntu 18.4.3 LST for image dataset training process. The loss function and optimizer has been employed as proposed model is binary cross entropy and adam. The CAE model generally

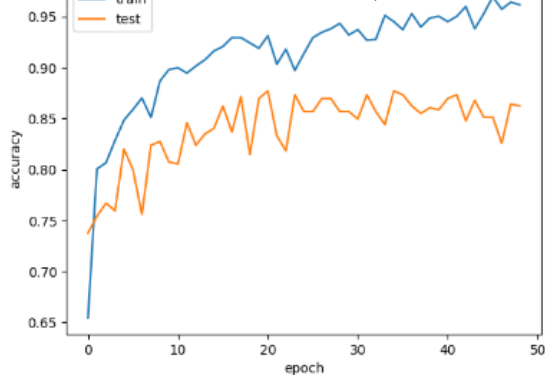


FIGURE 5 ACCURACY CURVE FOR CAE WITH LSTM METHOD

The figure 5 has illustrated the CAE with LSTM model accuracy in which accuracy for training is steady beyond 32 epochs as well as maintains the incremental accuracy from 92.45% to 96.20. Similarly in validation accuracy, the drastic change in accuracy and finally obtained with 86.32%. As the epochs increases the accuracy increases and slight decreases, whereas finally training accuracy is higher with 96.20% than testing accuracy is 86.32%.

Figure 6 has illustrated the CAE with LSTM model loss in training is from 0.6438 to 0.1172 and in the validation loss is 0.4263 to 0.3625 which is lesser than training since slow learning during initial epochs but epochs increases the loss get decreased. When the epoch gets increased, there is a reduction in loss from 0.6438 to 0.1172 which liable to define that TL have been occurred in minimizing the loss. In validation loss curve, the value of loss gets minimized from 0.4263 to 0.3625. Thus, the model is trained in the best mode for classifying the model with 96.20% accuracy.

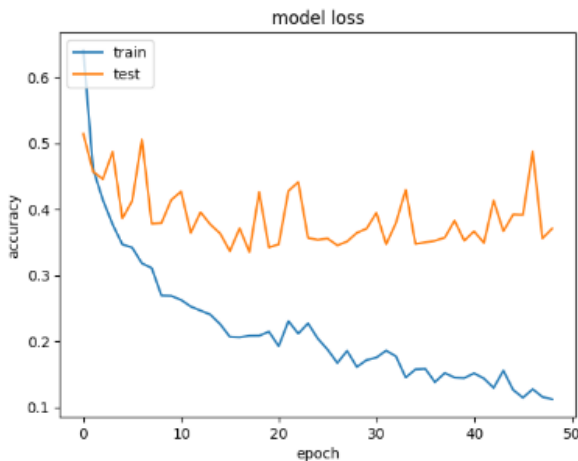


FIGURE 6 LOSS CURVE FOR CAE WITH LSTM METHOD

The suggested AE with CNN model defines the classification of no_tumor, meningioma_tumor, pituitary_tumor and glioma_tumor whereas Figures 7 and 8 show the associated model accuracy and loss for training and validation.

The figure 7 has illustrated the AE with CNN model accuracy in which accuracy for training is steady beyond 29 epochs as well

as validation accuracy from 92.55% to 94.15%. In validation accuracy, the drastic change in accuracy and finally obtained with 85.58%. As the epochs increases the accuracy increases and slight decreases, whereas finally training accuracy is higher with 94.15% than testing accuracy is 85.58%.

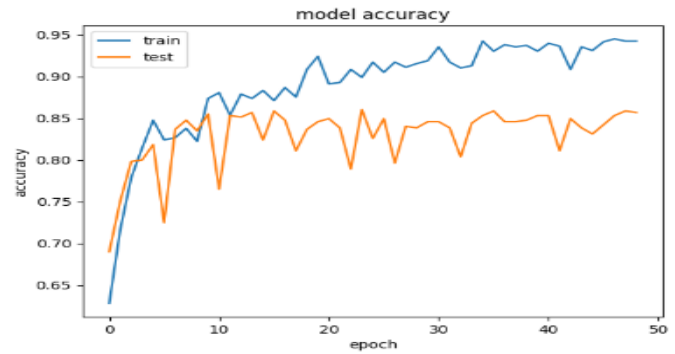


FIGURE 7 ACCURACY CURVE FOR AE WITH CNN METHOD

Figure 8 has illustrated the AE with CNN model loss in training is from 0.8156 to 0.1614 and in the validation loss is 0.5904 to 0.3801 which lesser than training since slow learning during initial epochs but epochs increases the loss get decreased. When the epoch gets increased, there is a reduction in loss from 0.8156 to 0.1614 which liable for defining TL that have been occur in minimizing the loss. In validation loss curve, the loss value gets minimized from 0.5918 to 0.3801. Thus, the model is trained in the best method for classifying the model with 94.15% accuracy.

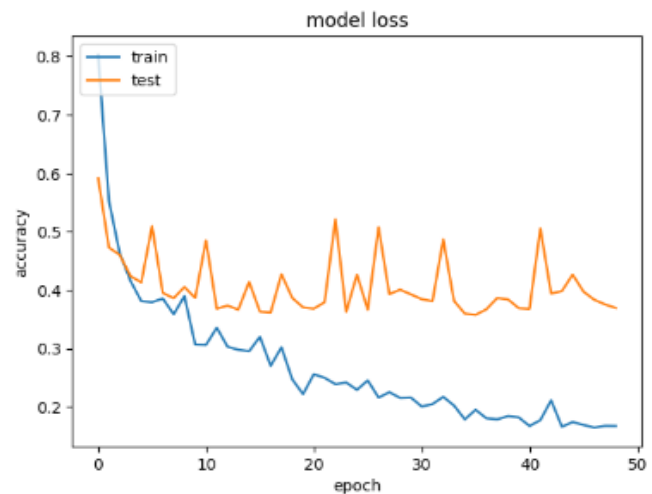


FIGURE 8 LOSS CURVE FOR AE WITH CNN METHOD

Table 2 illustrates the evaluation metrics for CAE with LSTM and AE with CNN in which accuracy and loss is determined through training and testing module.

TABLE 2 EVALUATION METRICS FOR CAE WITH LSTM AND AE WITH CNN

Evaluation Metrics	Model description	Training	Testing
Accuracy	AE with CNN	94.15	85.58
Loss	AE with CNN	0.1614	0.3801

Proceedings of the 6th International Conference on Mobile Computing and Communications (ICMCC-2021) DVD Part Number: CFP25US4-DVD; ISBN: 979-8-3315-2265-0	CAE with LSTM	96.20	86.32
Loss	AE with CNN	0.1614	0.3801
	CAE with LSTM	0.1172	0.3625

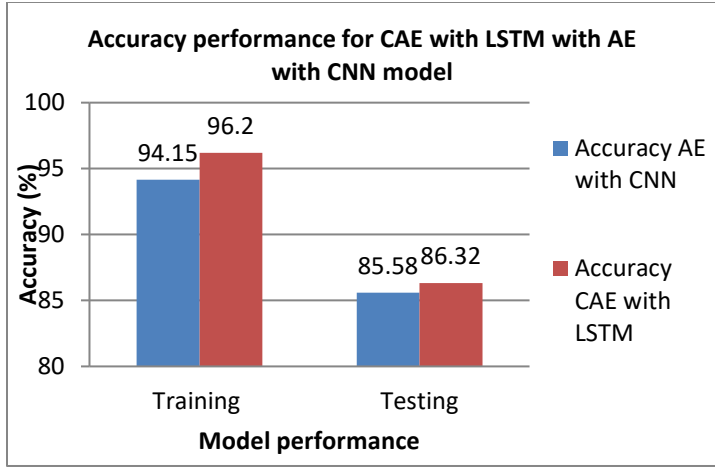


FIGURE 9 ACCURACY COMPARISONS OF CAE WITH LSTM AND AE WITH CNN

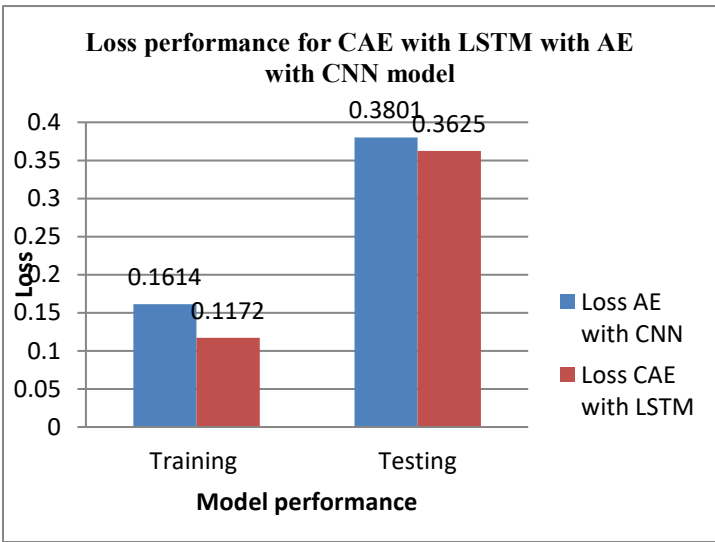


FIGURE 10 LOSS COMPARISONS OF CAE WITH LSTM AND AE WITH CNN

Figure 10 illustrates the model loss in training for AE with CNN is 0.1614 which is comparatively higher than CAE with LSTM is 0.1172 and in the case of validation loss for AE with CNN is 0.3801 is lesser than CAE with LSTM is 0.3625. Moreover, CAE with LSTM has generated high accuracy in training as well as testing module.

VI. CONCLUSION

This research has enhanced the performance of LSTM by introducing CAE technique on image classification tasks. The proposed study is to concentrate in using CAE as data preparation technique to reconstruct robust and compressed representations of features. In image classification models, the

RNN models and CNN models with CAE are typically taken into consideration. This research concentrated to prove that TL based method may leads to the highest performance than traditional and evaluated CAE with LSTM as 96.2% and 86.32% for training and testing results comparing with AE with CNN image classification models is 94.15% and 85.58%. Moreover, the proposed model is evaluated with AE with CNN model through the combination as well as incorporation of the BT image dataset. Therefore, the usage of CAE with LSTM for image classification methods which is a adequate layer in DL model selection for leading the reliable and robust experimental results. Thus, the prediction of BT detection is high accuracy in CAE with LSTM. In future, the prediction of BT has focused in improving validation prediction through hybrid model as TL with Bi-LSTM model for generating better validation in prediction of BT detection to create an application for detecting BT through MRI.

REFERENCES

1. Qureshi, S.A.; Raza, S.E.A.; Hussain, L.; Malibari, A.A.; Nour, M.K.; Rehman, A.U.; Al-Wesabi, F.N.; Hilal, A.M. Intelligent Ultra-Light Deep Learning Model for Multi-Class Brain Tumor Detection. *Appl. Sci.* **2022**, *12*, 3715.
2. Zahoor, M.M.; Qureshi, S.A.; Bibi, S.; Khan, S.H.; Khan, A.; Ghafoor, U.; Bhutta, M.R. A New Deep Hybrid Boosted and Ensemble Learning-Based Brain Tumor Analysis Using MRI. *Sensors* **2022**, *22*, 2726.
3. Arabahmadi, M.; Farahbakhsh, R.; Rezazadeh, J. Deep Learning for Smart Healthcare—A Survey on Brain Tumor Detection from Medical Imaging. *Sensors* **2022**, *22*, 1960.
4. Gore, D.V.; Deshpande, V. Comparative study of various techniques using deep Learning for brain tumor detection. In Proceedings of the 2020 IEEE International Conference for Emerging Technology (INCET), Belgaum, India, 5–7 June 2020; pp. 1–4.
5. Iorgulescu, J.B.; Sun, C.; Neff, C.; Cioffi, G.; Gutierrez, C.; Kruchko, C.; Ruhl, J.; Waite, K.A.; Negoita, S.; Hofferkamp, J.; et al. Molecular biomarker-defined brain tumors: Epidemiology, validity, and completeness in the United States. *Neuro-Oncology* **2022**, *24*, 1989–2000.
6. Gore, D.V.; Deshpande, V. Comparative study of various techniques using deep Learning for brain tumor detection. In Proceedings of the 2020 IEEE International Conference for Emerging Technology (INCET), Belgaum, India, 5–7 June 2020; pp. 1–4.
7. Soomro, T.A.; Zheng, L.; Afifi, A.J.; Ali, A.; Soomro, S.; Yin, M.; Gao, J. Image Segmentation for MR Brain Tumor Detection Using Machine Learning: A Review. *IEEE Rev. Biomed. Eng.* **2022**, *16*, 70–90. [CrossRef] [PubMed]
8. Yavuz, B.B.; Kanyilmaz, G.; Aktan, M. Factors affecting survival in glioblastoma patients below and above 65 years of age: A retrospective observational study. *Indian J. Cancer* **2021**, *58*, 210. [PubMed]
9. Fahmideh, M.A.; Scheurer, M.E. Pediatric brain tumors: Descriptive epidemiology, risk factors, and future directions. *Cancer Epidemiol. Prev. Biomark.* **2021**, *30*, 813–821. [CrossRef]
10. Nodirov, J.; Abdusalomov, A.B.; Whangbo, T.K. Attention 3D U-Net with Multiple Skip Connections for Segmentation of Brain Tumor Images. *Sensors* **2022**, *22*, 6501.
11. Ahuja, S.; Panigrahi, B.K.; Gandhi, T.K. Enhanced performance of Dark-Nets for brain tumor classification and segmentation using colormap-based superpixel techniques. *Mach. Learn. Appl.* **2022**, *7*, 100212.
12. Gu X, Shen Z, Xue J, Fan Y, Ni T. Brain tumor MR image classification using convolutional dictionary learning with local constraint. *Front Neurosci* **2021**;15.
13. Diaz-Pernas FJ, Martinez-Zarzuola M, Anton-Rodriguez M. A deep learning approach for brain tumor classification and segmentation using a multiscale convolutional neural network. *Healthcare* **2021**;9(2):1015–36.
14. Taher, H.Z., Gamel SA, El-Kenawy E-SM, Alharbi AH, Doaa SK, Abdelhameed I, Fatma M. Brain tumor detection and classification

15. Abdul Hayum, A., Jaya, J., Paulchamy, B., & Sivakumar, R. (2023). A modified recurrent neural network (MRNN) model for and breast cancer classification system. *Automatika*, 64(4), 1193–1203. <https://doi.org/10.1080/00051144.2023.2253064>
16. Nazir, M., Shakil, S., & Khurshid, K. 2021. Role of deep learning in brain tumor detection and classification (2015 to 2020): A review. *Computerized Medical Imaging and Graphics*, 91, 101940.
17. Satpute, B. S., Kale, A., Dhande, D., Kuber, H., & Chore, S. 2020. Brain Tumor Detection using Deep Learning Technique.
18. Kabir, M. A. (2020). Automatic brain tumor detection and feature extraction from MRI image. *GSJ*, 8(4).
19. Hameed, Z., Zahia, S., Garcia-Zapirain, B., Aguirre, J. J. & Vanegas, A. M. Breast cancer histopathology image classification using an ensemble of deep learning models. *Sensors* <https://doi.org/10.3390/s20164373> (2020).
20. Yan, R. et al. Breast cancer histopathological image classification using a hybrid deep neural network. *Methods* <https://doi.org/10.1016/j.ymeth.2019.06.014> (2020).
21. Feng, Y., Zhang, L. & Mo, J. Deep manifold preserving autoencoder for classifying breast cancer histopathological images. *IEEE/ ACM Trans. Comput. Biol. Bioinform.* <https://doi.org/10.1109/TCBB.2018.2858763> (2020).
22. Nguyen, H. D., Vu, X. S. & Le, D. T. Modular graph transformer networks for multi-label image classification. In 35th AAAI Conference on Artificial Intelligence, AAAI 2021, Vol. 10B. <https://doi.org/10.1609/aaai.v35i10.17098> (2021).
23. Wang, P. et al. Automatic classification of breast cancer histopathological images based on deep feature fusion and enhanced routing. *Biomed. Signal Process. Control* <https://doi.org/10.1016/j.bspc.2020.102341> (2021).
24. Thilagaraj, M., Arunkumar, N. & Govindan, P. Classification of breast cancer images by implementing improved DCNN with artificial fish school model. *Comput. Intell. Neurosci.* <https://doi.org/10.1155/2022/6785707> (2022).
25. Hong, D. et al. SpectralFormer: Rethinking hyperspectral image classification with transformers. *IEEE Trans. Geosci. Remote Sens.* <https://doi.org/10.1109/TGRS.2021.3130716> (2022).
26. Liu, Y., Dou, Y., Jin, R., Li, R. & Qiao, P. Hierarchical learning with backtracking algorithm based on the Visual Confusion Label Tree for large-scale image classification. *Vis. Comput.* 38(3), 897–917. <https://doi.org/10.1007/s00371-021-02058-w> (2022).